

A Possible New Population of Sources with Extreme X-Ray / Optical Ratios^{1,2}

Anton M. Koekemoer³, D. M. Alexander^{4,5}, F. E. Bauer⁴, J. Bergeron⁶, W. N. Brandt⁴, E. Chatzichristou⁷, S. Cristiani⁸, S. M. Fall³, N. A. Grogin⁹, M. Livio³, V. Mainieri¹¹, L. Moustakas³, P. Padovani^{3,10}, P. Rosati¹¹, E. J. Schreier¹², C. M. Urry⁷

ABSTRACT

We describe a possible new class of X-ray sources that have robust detections in ultra-deep *Chandra* data, yet have no detections at all in our deep multi-band GOODS *Hubble Space Telescope (HST)* ACS images, which represent the highest quality optical imaging obtained to date on these fields. These extreme X-ray / Optical ratio sources (“EXO”s) have values of F_X/F_{opt} at least an order of magnitude above those generally found for other AGN, even those that are harbored by reddened hosts. We thus infer two possible scenarios: (1) if these sources lie at redshifts $z \lesssim 6$, then their hosts need to be exceedingly underluminous, or more reddened, compared with other known sources; (2) if these sources lie above $z \sim 6 - 7$, such that even their Lyman- α emission is redshifted out of

^{1,2}Based on observations obtained with the NASA/ESA *Hubble Space Telescope*, which is operated by the Association of Universities for Research in Astronomy, Inc., under NASA contract NAS 5-26555, and at the European Southern Observatory, Chile (164.O-0561, 169.A-0725, 267.A-5729, 66.A-0451, 68.A-0375).

³Space Telescope Science Institute, 3700 San Martin Drive, Baltimore, MD 21218, USA

⁴Penn State University, 525 Davey Lab, University Park, PA 16802 USA

⁵Institute of Astronomy, Madingley Road, Cambridge, CB3 0HA, UK

⁶Institut d’Astrophysique de Paris, 98bis Bd Arago, F-75014 Paris, France

⁷Department of Physics (JWG 460), Yale University, P.O. Box 208121, New Haven CT 06520-8121, USA

⁸INAF-Osservatorio Astronomico, via Tiepolo 11, I-34131 Trieste, Italy

⁹Department of Physics and Astronomy, Johns Hopkins University, Baltimore, MD 21218, USA

¹⁰ESA Space Telescope Division

¹¹European Southern Observatory, Karl-Schwarzschild-Str. 2, Garching D-85748, Germany

¹²Associated Universities, Inc., 1400-16th St, NW, Ste 730, Washington, DC 20036, USA

the bandpass of our ACS z_{850} filter, then their optical and X-ray fluxes can be accounted for in terms of relatively normal $\sim L_*$ hosts and moderate-luminosity AGN.

Subject headings: X-rays: galaxies — galaxies: active — galaxies: evolution — galaxies: high-redshift — surveys

1. Introduction

A key question in astrophysics concerns the evolution of active galactic nuclei (AGN) during the “quasar epoch” ($z \sim 2 - 3$) and at higher redshifts, where their space density declines (Fan et al. 2001, 2003; Barger et al. 2003). Their evolution appears to track the star formation rate (e.g., Steidel et al. 1999), thereby suggesting an empirical link between galaxy growth and AGN fuelling. A connection between galaxies and AGN is also suggested by the black hole / bulge mass relationship (Ferrarese & Merritt 2000; Gebhardt et al. 2000).

A powerful tool to investigate the physical nature of such relationships is AGN X-ray emission, which above a few keV can penetrate obscuration around AGN. Ultra-deep X-ray surveys with *Chandra* on the Hubble Deep Field North (HDF-N; Brandt et al. 2001), and Chandra Deep Field South (CDF-S; Giacconi et al. 2002) are sufficiently sensitive to reveal AGN beyond the tentative reionization epoch ($z \sim 6 - 7$, Fan et al. 2001, 2003), where optical information is no longer available. These surveys also probe more numerous, lower-luminosity AGN at $z \sim 3 - 6$, where ultra-deep optical and near-IR imaging can constrain their properties.

In this paper we describe a sample of sources with extreme X-ray / Optical flux ratios (or “EXO”s), that are robustly detected (25 – 89 counts) in the 2 Msec HDF-N and reprocessed 1 Msec CDF-S main catalogs (Alexander et al. 2003). They are also detected in near-IR *JHK* imaging, but completely undetected in our deep GOODS *HST*/ACS survey, which to date is the most sensitive and detailed optical imaging of these fields (Giavalisco et al. 2003). We discuss various possible interpretations for these objects. Throughout this paper we adopt $H_0 = 70 \text{ km s}^{-1} \text{ Mpc}^{-1}$, $\Omega_M = 0.3$, and $\Omega_\Lambda = 0.7$.

2. Observations and Sample Description

We began by matching the X-ray catalogs (Alexander et al. 2003) to our ACS z_{850} catalogs (Giavalisco et al. 2003); details are in Koekemoer et al. (2003, in preparation) and

Bauer et al. (2003, in preparation). The matched sources are mostly moderate-luminosity AGN at $z \sim 0.5 - 4$, or star-forming galaxies at $z \lesssim 0.5 - 1$ (e.g., Hornschemeier et al. 2001; Schreier et al. 2001; Alexander et al. 2001; Koekemoer et al. 2002).

The remaining sources were inspected in detail by overlaying X-ray contours on the z_{850} and the combined $B_{435}+V_{606}+i_{775}+z_{850}$ images. Most of these had faint optical counterparts, below the formal $10\text{-}\sigma$ z_{850} catalog threshold or undetected in z_{850} but detected in another band (perhaps high equivalent width Lyman- α emitters). Detection in z_{850} or bluer bands suggests these sources are at $z \lesssim 6$ (Barger et al. 2003; Cristiani et al. 2003).

Finally, there remained sources with no ACS counterparts within $2''.4$ ($\gtrsim 10$ times the positional uncertainty) in z_{850} and the combined $B_{435}+V_{606}+i_{775}+z_{850}$ images, despite robust detections in the X-ray main catalogs (25 – 89 counts). We focus on CDF-S where we have complete ACS and near-IR coverage; HDF-N sources will be discussed separately (Koekemoer et al. 2003, in preparation). Five of these 7 CDF-S sources have fairly well behaved X-ray exposure maps; the other two are still detected in *JHK* thus are likely also real. The sources are also at a wide range of off-axis angles in the *Chandra* image. We computed z_{850} upper limits from the pixel r.m.s. ($0.0017 - 0.0024$ counts s^{-1} pixel $^{-1}$), integrated over a $0''.2 \times 0''.2$ aperture (4×4 ACS-pixel box), to yield $3\text{-}\sigma$ upper limits¹¹ of $z_{850} \sim 27.9 - 28.4$ (AB magnitudes).

3. “EXO”s: Extreme X-ray / Optical Ratio Sources

The 7 sources with no ACS counterparts are shown in Figure 1. We carried out photometry at the X-ray positions, and present the ACS upper limits and near-IR detections in Table 1. To further investigate the nature of these sources, we examine the relationship between their X-ray and optical fluxes (e.g., Maccacaro et al. 1988; Stocke et al. 1991). In Figure 2 we plot $F_{0.5-8\text{keV}}$ versus z_{850} for all the X-ray sources, including the ACS non-detections, also showing lines of constant F_X/F_{opt} (derived from z_{850}). At soft X-ray energies this ratio is complicated by absorption and thermal gas emission (e.g., Beuermann et al. 1999) but these no longer dominate above a few keV, which is redshifted into the soft band for $z \gtrsim 1 - 2$. Sources with $F_X/F_{\text{opt}} \gtrsim 0.1 - 10$ are generally identified with AGN; these deep X-ray data also reveal normal galaxies and starbursts (e.g., Hornschemeier et al. 2003) with F_X/F_{opt} extending a few orders of magnitude below AGN, but at $z_{850} \gtrsim 24$ these are lost from the X-ray sample and the AGN dominate.

¹¹Using the same zeropoints as Giavalisco et al. (2003).

Figure 2 also reveals that our z_{850} -undetected objects occupy the high end of the F_X/F_{opt} plane, above most of the detected optically faint sources. This is interesting since it is not expected *a priori* that optically undetected objects should have strong X-ray flux. We also plot our measured ACS magnitudes for CDF-S sources reported as undetected in ground-based data by Yan et al. (2003), and show Extremely Red Objects (EROs) from previous studies (Alexander et al. 2002; Stevens et al. 2003).

In Figure 3 we plot F_X/F_{opt} against $z_{850} - K$; the normal galaxies and starbursts with $F_X/F_{\text{opt}} \lesssim 0.1 - 1$ are blue, while the only objects with $z_{850} - K > 4$ are those with high F_X/F_{opt} (see also Brusa et al. 2002; Cagnoni et al. 2002). Not *all* the high F_X/F_{opt} objects are red; some are blue, with $z_{850} - K \sim 0 - 2$, and are likely unobscured AGN. However, at high F_X/F_{opt} we also find the reddest objects, with most of our undetected z_{850} sources at the extreme end with $z_{850} - K \gtrsim 4.2 - 6.2$.

4. Possible Constituents of the “EXO” Population

We now examine various possibilities for these sources in order to explain: (1) deep optical non-detection; (2) robust X-ray detection; and (3) extremely red colors. We rule out main-sequence stars as these typically have $F_X/F_{\text{opt}} \sim 10^{-5} - 0.1$ (e.g., Stocke et al. 1991). More exotic galactic sources include low-mass X-ray binaries, cataclysmic variables, or neutron stars, which generally have $L_X \sim 10^{30} - 10^{35}$ erg s⁻¹ (e.g., Verbunt & Johnston 1996 and references therein). At distances $\sim 10 - 100$ kpc they would have X-ray fluxes $\lesssim 10^{-14}$ erg s⁻¹ cm⁻², consistent with what is observed. However, the number of sources in our small survey area would imply total counts $\sim 10^4 - 10^5$ times above what is known for our galaxy (e.g. Howell & Szkody 1990; Alexander et al. 2001). Thus we turn to an extragalactic origin for the *EXOs*.

Low-luminosity galaxies can host relatively luminous X-ray sources, for example the local dwarf NGC 4395 ($M_B \sim -16.5$) with a central X-ray source $L_{2-10\text{keV}} \sim 3 \times 10^{38}$ erg s⁻¹ (Ho et al. 2001). However, such objects do not have the extremely red colors of our sources. Moreover, our z_{850} limits would imply a distance modulus $\gtrsim 45.3$ mag, hence $L_X \gtrsim 3 \times 10^{42} - 8 \times 10^{43}$ erg s⁻¹, at least 10^4 times above those for such dwarfs locally. It would be highly interesting if the *EXOs* were low-luminosity dwarfs with such extreme AGN, but since we know of no local analogs, we explore other alternatives.

4.1. Evolved Galaxies

A possible alternative is that the *EXOs* may be at moderate redshifts and extremely evolved. At $z \sim 1, 2, 3, 4, 5, 6$, the oldest possible populations (5.7, 3.2, 2.1, 1.5, 1.2, 0.9 Gyr) would have observed colors $z_{850} - K \sim 1, 4, 4.5, 3.5, 3.2, 3$ respectively, for a single-burst model with 0.3 solar metallicity (Charlot & Bruzual 2003, in preparation). At least $\sim 1 - 2$ magnitudes of extinction would be required since we observe no UV excess. These properties are comparable to those derived for other X-ray ERO's (e.g., Alexander et al. 2002; Brusa et al. 2002; Stevens et al. 2003). However, it is interesting to note that the *K*-band magnitudes are ~ 100 times too low compared to what is needed to place these objects on the $M_{BH} - \sigma$ relation (see Woo & Urry 2002).

4.2. Dusty Galaxies

We next explore the amount of dust needed to achieve the high $z_{850} - K$ colors. If these sources were local ($z \lesssim 0.1$), then $z_{850} - K \gtrsim 4.5$ would imply $A_V \gtrsim 10 - 14$ (Rieke & Lubofsky 1985; Calzetti 1997), depending on the stellar populations. This would require a column $N_H \gtrsim 2 - 5 \times 10^{22} \text{ cm}^{-2}$ ratio, which is too high for the observed soft X-ray fluxes unless we invoke a highly interesting scenario where the AGN is unobscured while the rest of the galaxy is completely obscured.

At higher redshifts, the A_V limits decrease since z_{850} and *K* sample bluer rest-frame wavelengths. Between $z \sim 1 - 2.5$ we infer $A_V \gtrsim 5 - 2$ respectively, comparable to similar objects discussed by Alexander et al. (2002); Smail et al. (2002); Stevens et al. (2003), and Yan et al. (2003). Again it is interesting that the *EXO* host luminosities at these redshifts, from their *K* magnitudes, would place them at least 2 orders of magnitude away from the $M_{BH} - \sigma$ relation implied by their X-ray fluxes, suggesting atypical accretion rates (Woo & Urry 2002).

4.3. High-Redshift Lyman Break Galaxies

Finally we investigate the possibility that these sources are at high enough redshifts to move the Lyman break out of the z_{850} filter. Yan et al. (2003) investigated similar possibilities for their CDF-S sources undetected in ground-based *R* imaging but detected with ISAAC. We have in fact detected their sources in our ACS z_{850} data (Figure 2) and agree with them that those sources are unlikely to be at $z \gtrsim 5$. However, their sources are the only ones with F_X/F_{opt} comparable to our *EXOs*. Thus, if the *EXOs* belong to the same population as the

Yan et al. (2003) sources, then their distance modulus is $\gtrsim 1.5 - 2$ magnitudes higher. If the Yan et al. (2003) sources are luminous E/S0 galaxies with $z \sim 1 - 2.5$, this would translate to $z \sim 2.5 - 6$ for the *EXO* population. The other possibility considered by Yan et al. (2003) is that their sources may be higher redshift AGN up to $z \sim 3 - 5$, depending on extinction details. If *EXO*'s are the high redshift extension of this population, this would place them at $z \sim 6 - 10$. In this case, their host galaxy absolute magnitudes (from our *K*-band data) would be -20 to -21 , comparable to $\sim L_*$ luminosities, while their X-ray luminosities would be $\sim 2 - 6 \times 10^{44}$ erg s $^{-1}$. These are not unusually high luminosities for AGN, and may be consistent with a high-redshift extension of moderate-luminosity AGN at $z \sim 3 - 5$ (eg Cristiani et al. 2003).

5. Conclusions

We have examined various possible explanations for a population of objects that have extreme X-ray / Optical ratios (“*EXO*”s), being robustly detected in the Chandra data in CDF-S and HDF-N, yet completely undetected in our deep multi-band $B_{435} + V_{606} + i_{775} + z_{850}$ ACS images, which represent the most sensitive optical imaging obtained to date on these fields. In particular, the lack of detections even in the z_{850} band suggests one of two possible scenarios: (1) if these sources lie at $z \lesssim 6 - 7$, then their hosts are unusually underluminous, or more reddened, compared with other known AGN hosts (even other ERO’s); (2) if these sources lie above $z \sim 6 - 7$, such that even their Lyman- α emission is redshifted out of the ACS z_{850} bandpass, then their optical and X-ray fluxes can be accounted for in terms of $\sim L_*$ hosts and moderate-luminosity AGN. Deep near-IR spectroscopic observations will help further elucidate their nature.

Partial support for this work was provided by NASA through grant number HST-GO-09583.01-96A from the Space Telescope Science Institute, which is operated by the Association of Universities for Research in Astronomy, under NASA contract NAS 5-26555. Support for this work, part of the *Space Infrared Telescope Facility (SIRTF)* Legacy Science program, was also provided by NASA through Contract Number 1224666 issued by the Jet Propulsion Laboratory, California Institute of Technology under NASA contract 1407. We thank the referee for a speedy review and for valuable suggestions that helped to improve this paper. AMK wishes to thank Mark Dickinson for insightful discussions, and Harry Ferguson for thorough comments on the manuscript. DMA acknowledges the generous support provided by a Royal Society University Research Fellowship. DMA, FEB and WNB also wish to thank NSF CAREER award AST-9983783.

REFERENCES

- Alexander, D., Brandt, W. N., Hornschemeier, A., Garmire, G., Schneider, D., Bauer, F. & Griffiths, R. 2001, AJ 122, 2156
- Alexander, D., Vignali, C., Bauer, F., Brandt, W. N., Hornschemeier, A., Garmire, G., & Schneider, D. 2002, AJ 123, 1149
- Alexander, D., Bauer, F., Brandt, W. N., Schneider, D., Hornschemeier, A., Vignali, C., Barger, A., Broos, P., Cowie, L., Garmire, G., Townsley, L., Bautz, M., Chartas, G., & Sargent, W. 2003, astro-ph/0304392
- Barger, A., Cowie, L., Capak, P., Alexander, D., Bauer, F., Brandt, W. N., Garmire, G., & Hornschemeier, A. 2003, ApJ 584, L61
- Beuermann, K., Thomas, H.-C., Reinsch, K., Schwobe, A. D., Trümper, J., & Voges, W. 1999, A&A 347, 7
- Brandt, W. N., Hornschemeier, A., Alexander, D., Garmire, G., Schneider, D., Broos, P., Townsley, L., Bautz, M., Feigelson, E., & Griffiths, R. 2001, AJ 122, 1
- Brusa, M., Comastri, A., Daddi, E., Cimatti, A., Mignoli, M., & Pozzetti, L. 2002, ApJ 581, L89
- Cagnoni, I., Elvis, M., Kim, D. W., Nicastro, F., & Celotti, A. 2002, ApJ 579, 148
- Calzetti, D. 1997, AJ 113, 162
- Cristiani, S. et al. 2003, ApJL, submitted
- Fan, X. et al. 2001, AJ 121, 54
- Fan, X. et al. 2003, AJ 125, 1649
- Ferrarese, L. & Merritt, D. 2000, ApJ, 539, 9
- Gebhardt, K., Kormendy, J., Ho, L., Bender, R., Bower, G. Dressler, A., Faber, S., Filippenko, A., Green, R., Grillmair, C., Lauer, T., Magorrian, J., Pinkney, J., Richstone, D., & Tremaine, S. 2000, ApJ, 539, 13
- Giacconi, R., Zirm, A., Wang, J. X., Rosati, P., Nonino, M., Tozzi, P., Gilli, R., Mainieri, V., Hasinger, G., Kewley, L., Bergeron, J., Borgani, S., Gilmozzi, R., Grogin, N., Koekemoer, A., Schreier, E., Zheng, W. & Norman, C. 2002, ApJS 139, 369
- Giavalisco, M. et al. 2003, ApJL, submitted
- Ho, L., Feigelson, E. D., Townsley, L., Sambruna, R., Garmire, G., Brandt, W. N., Filippenko, A., Griffiths, R., Ptak, A., & Sargent, W. 2001, ApJ 549, L51
- Hornschemeier, A. E., et al. 2001, ApJ 554, 742

- Howell, S. B. & Szkody, P. 1990, *ApJ* 356, 623
- Koekemoer, A. M., Grogan, N. A., Schreier, E. J., Giacconi, R., Gilli, R., Kewley, L., Norman, C., Zirm, A., Bergeron, J., Rosati, P., Hasinger, G., Tozzi, P., & Marconi, A. 2002, *ApJ*, 567, 657
- Maccacaro, T., Gioia, I., Wolter, A., Zamorani, G., & Stocke, J. 1988, *ApJ* 326, 680
- Rieke, G. H. & Lebofsky, M. J. 1985, *ApJ* 288, 618
- Schreier, E., Koekemoer, A., Grogan, N., Giacconi, R., Gilli, R., Kewley, L.; Norman, C., Hasinger, G., Rosati, P., Marconi, A., Salvati, M., & Tozzi, P. 2001, *ApJ*, 560, 127
- Smail, I., Owen, F., Morrison, G., Keel, W., Ivison, R., & Ledlow, M. 2002, *ApJ* 581, 844
- Steidel, C., Adelberger, K., Giavalisco, M., Dickinson, M., & Pettini, M. 1999, *ApJ* 519, 1
- Stevens, J., Page, M., Ivison, R., Smail, I., Lehmann, I., Hasinger, G. & Szokoly, G. 2003, *astro-ph/0302289*
- Stocke, J., Morris, S., Gioia, I., Maccacaro, T., Schild, R., Wolter, A., Fleming, T., & Henry, J. 1991, *ApJS*, 76, 813
- Verbunt, F. & Johnston, H. M. 1996, in *ASP Conf. Ser. 90, The Origins, Evolution, and Destinies of Binary Stars in Clusters*, ed. E. F. Milone & J.-C. Mermilliod, 300
- Woo, J.-H. & Urry, C. M. 2002, *ApJ* 579, 530
- Yan, H., Windhorst, R., Röttgering, H., Cohen, S., Odewahn, S., Chapman, S., & Keel, W. 2003, *ApJ* 585, 67

Fig. 1.— The 7 CDF-S X-ray sources with no ACS counterparts, also showing the SOFI *JHK* detections. Each panel is 15'' on a side. Contours show 0.5 – 8 keV *Chandra* data, starting at 1,2,3- σ , and doubling thereafter. For the full image, see <http://www.stsci.edu/~koekemoe/goods-exo/>

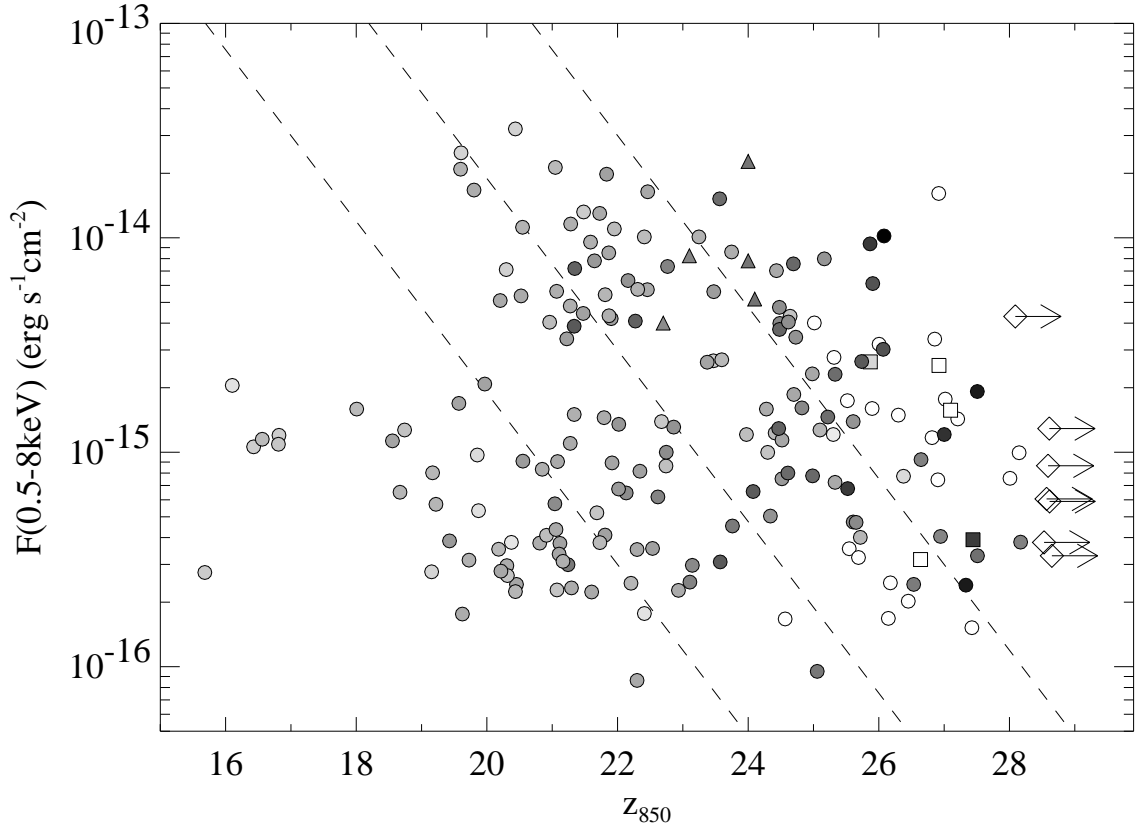


Fig. 2.— Total X-ray flux (0.5 – 8 keV) against z_{850} magnitude for all the X-ray sources, including those unidentified in z_{850} (indicated by diamonds with arrows). Lines indicate $F_X/F_{\text{opt}} = 0.1, 1, 10$. Symbol shading shows the $z_{850} - K$ colour of each source, ranging from light to dark for $z_{850} - K \sim 0 - 5$. White symbols (no shading) were undetected in K . Squares show our measured ACS magnitudes for sources reported as undetected in ground-based data by Yan et al. (2003), and triangles indicate X-ray selected EROs in the Lockman Hole (Stevens et al. 2003).

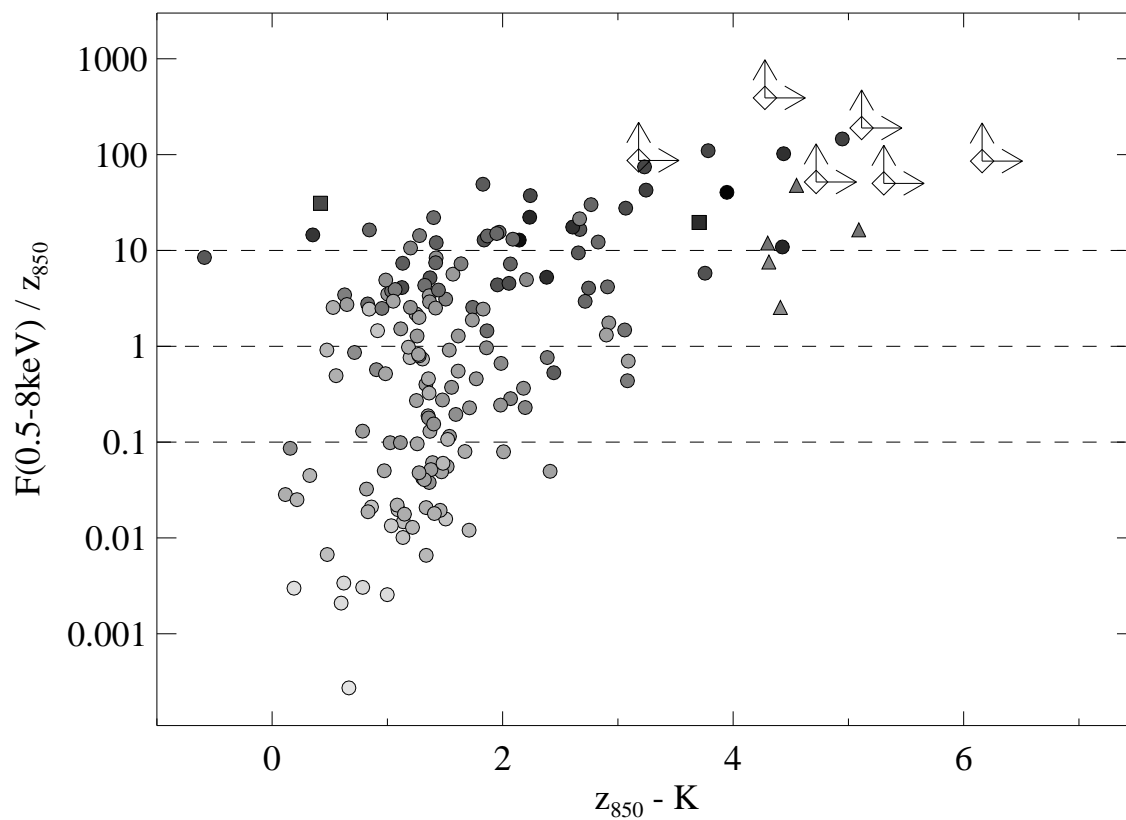


Fig. 3.— Ratio of $F_{0.5-8\text{keV}}$ to z_{850} for all the X-ray sources, plotted against $z_{850} - K$. Symbol shapes are as in Figure 2; however shading represents z_{850} , fainter sources being darker. Normal galaxies and starbursts ($F_X/F_{\text{opt}} \lesssim 0.1 - 1$) are relatively blue, and that the only redder objects are those with higher F_X/F_{opt} .

Table 1. Optically Undetected X-Ray Sources

R.A. ^a (J2000)	Dec. ^a (J2000)	Total counts (0.5 – 8 keV)	$F_{0.5-8\text{keV}}$ ($\text{erg s}^{-1}\text{cm}^{-2}$)	z_{850}	J	H	K
03 32 08.39	–27 40 47.0	89_{-14}^{+15}	4.3×10^{-15}	>27.9	25.2 ± 1.3	23.3 ± 0.2	24.8 ± 1.1
03 32 08.89 ^b	–27 44 24.3	27_{-8}^{+9}	3.8×10^{-16}	>28.3	>25.9	24.8 ± 0.5	23.8 ± 0.6
03 32 13.92	–27 50 00.7	44_{-8}^{+9}	6.1×10^{-16}	>28.3	23.9 ± 0.4	22.7 ± 0.1	22.4 ± 0.2
03 32 20.36	–27 42 28.5	42_{-10}^{+11}	8.7×10^{-16}	>28.3	>25.9	>25.1	>25.0
03 32 25.83	–27 51 20.3	25_{-6}^{+7}	3.3×10^{-16}	>28.4	>25.9	>25.1	23.3 ± 0.4
03 32 33.14	–27 52 05.9	44_{-7}^{+9}	5.9×10^{-16}	>28.4	25.7 ± 1.1	24.8 ± 0.5	25.4 ± 1.5
03 32 51.64	–27 52 12.8	45_{-9}^{+11}	1.3×10^{-15}	>28.4	>25.9	24.1 ± 0.3	23.5 ± 0.6

^aPositions for the X-ray sources, from Alexander et al. (2003).

^bThis source was also optically undetected by Yan et al. (2003); note that we detect their other sources in our z_{850} data.

This figure "f1.jpg" is available in "jpg" format from:

<http://arxiv.org/ps/astro-ph/0306407v1>